analytical chemistry

Article

pubs.acs.org/ac

# Method for Time-Resolved Monitoring of a Solid State Biological Film Using Photothermal Infrared Nanoscopy on the Example of Poly-L-lysine

Georg Ramer, Anna Balbekova, Andreas Schwaighofer, and Bernhard Lendl*

Vienna University of Technology, Institute for Chemical Technologies and Analytics, Getreidemarkt 9/164 UPA, 1060 Vienna, Austria

Supporting Information

**ABSTRACT:** We report time-resolved photothermal infrared nanoscopy measurements across a spectral range of more than 100 $cm^{-1}$ (1565 $cm^{-1}$ to 1729 $cm^{-1}$) at nanoscale spatial resolution. This is achieved through a custom-built system using broadly tunable external cavity quantum cascade lasers in combination with a commercially available atomic force microscope. The new system is applied to the analysis of conformational changes of a polypeptide (poly-L-lysine) film upon temperature-induced changes of the humidity in the film. Changes of the secondary structure from $\beta$-sheet to $\alpha$-helix could be monitored at a time resolution of 15 s per spectrum. The time-resolved spectra are well comparable to reference measurements acquired with conventional Fourier transform infrared microscopy.

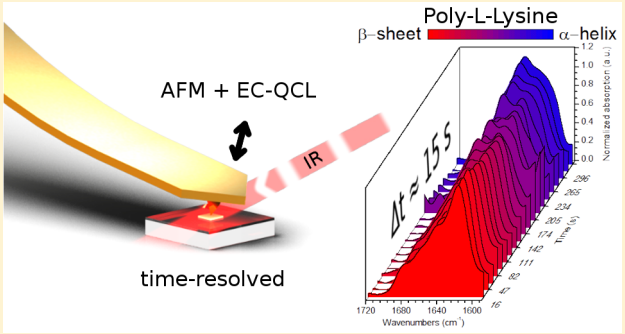


Infrared (IR) spectroscopy is an advantageous, nondestructive and label-free technique for chemical analysis. Fourier transform infrared (FTIR) spectroscopy is a commonly used method for the analysis of biological samples,[1] in particular for proteins and peptides.[2,3] Recently, IR microscopy showed great promise in the medical field for the analysis of human tissue and cell films.[1,4] However, the spatial resolution of IR optical microscopes is limited to the scale of several microns,[5] when using far-field techniques, where either the detector (aperture) or the light source is placed at distances of more than one wavelength from the sample. This practically precludes imaging of structures smaller than the employed wavelengths. That limitation can be overcome with near-field techniques—either detector (aperture) or light source placed at distances less than one wavelength from the sample—and the spatial resolution can be greatly enhanced.

Recent developments in the area of near-field imaging have made it possible to record IR spectra and images at a nanoscale spatial resolution. Currently, there are two well-established techniques allowing performance of such high-resolution measurements: one is a scattering scanning near-field technique based on pseudoheterodyne detection in the far-field (scattering scanning near-field optical microscopy, sSNOM);[6,7] the other uses thermal expansion of the sample upon illumination with pulsed IR light.[8,9] The latter method is often called AFMIR (atomic force microscope−infrared or induced resonance) or PTIR (photothermal induced resonance). Both methods have in common that an AFM cantilever is used to obtain high lateral spatial resolution. Both of them are capable of spatial resolution in IR imaging down to about 20 nm,[10,11] while still providing absorption spectra very similar to those acquired in conventional, far-field IR spectroscopy. The least sample amount detected for both methods is a single monolayer.[11,12] A main difference in performance of the near-field techniques is that sSNOM only detects analytes in the enhanced electromagnetic field around the cantilever tip, whereas AFMIR also perceives analytes at a distance of one micrometer or more beneath the sample surface.[13] PTIR has been applied for the analysis of micro-organisms, cells and other biological materials[14,15] and for the analysis of polymer films.[16] Other applications of PTIR include imaging of the modes of plasmonic resonators[17] and the analysis of micron-sized crystals.[18] sSNOM has been used for analyzing plasmonic modes in graphene[19−21] and in metallic infrared antennas.[22] It has been established as a technique for the analysis of polymer films[23] and is also able to perform spectroscopy on single protein complexes.[12]

In recent years imaging resolution and sensitivity have been improved at a rapid pace for sSNOM and PTIR; however, the majority of works addressed static systems only, i.e. systems that do not exhibit any induced changes during the measurement. Wagner et al.[21,24] demonstrated time-resolved sSNOM in repeatable events, i.e. events that can be repeated and reproduced many times without exchanging the sample. In

**Received:** January 19, 2015
**Accepted:** March 26, 2015
**Published:** March 26, 2015





DOI: 10.1021/acs.analchem.5b00241
*Anal. Chem.* 2015, 87, 4415−4420

these pump−probe experiments, time resolutions down to 200 fs via changing the delay line of the pump pulse were achieved at a spectral range of 400 $cm^{-1}$. Spectral resolution was obtained via an interferometer and Fourier transform. In order to be able to apply this technique, the observed event has to be repeatable in exactly the same way for each interferogram position at each time step.

For nonrepeatable events, time-resolved measurements of the local IR absorption at a single wavelength can be achieved with both currently commercially available sSNOM and PTIR instruments. For such measurements, the cantilever is kept in place while the sample is irradiated by IR light pulses. However, single wavelength information is often not sufficient for IR spectroscopy. A graphic example is the investigation of the secondary structure changes of proteins. Via exclusive monitoring of the amide I band at either 1650 $cm^{-1}$ ($\alpha$-helix) or 1633 $cm^{-1}$ ($\beta$-sheet),[25] the change from $\alpha$-helix to $\beta$-sheet is easily mistaken for a decrease or increase, respectively, in the total protein concentration. Monitoring of the entire amide I region provides a complete picture of the ongoing transformations of the protein—as will be demonstrated in this work.

Instead of collecting the absorbance at a single wavenumber, in this study we present the use of an external cavity quantum cascade laser (EC-QCL) in combination with a PTIR setup to measure the IR absorption across a wavenumber range of more than 100 $cm^{-1}$. This new method only needs a single repetition of the event to acquire time-resolved spectra. To achieve this objective, a Daylight solutions EC-QCL is used in its scan mode. Here the grating is swept in one continuous motion to cover the whole tuning range of the source in a short time. When using the scan mode, it is crucial to know the relation between the time that has passed since the start of the scan and the wavelength emitted by the laser. This relation was determined for the laser used in this work through characterization with a step-scan FTIR spectrometer.[26,27]

In this paper, we demonstrate the viability of our measurement scheme by monitoring the secondary structure change of a poly-L-lysine (PLL) thin film. This particular polypeptide was chosen, because its secondary structure changes depending on the hydration level of the film.[28] The conformational changes can therefore be introduced at comparatively soft conditions: at ambient pressure, without aggressive chemicals and at temperatures near room temperature. Since the secondary structure change is reversible, a single sample could be reused for several experiments. This, however, is not a necessity for the method introduced in this work. During experiments, the hydration was changed via the relative humidity above the film. The humidity was controlled by changing the temperature of the film in a humid environment. PLL is widely used as a model substance for proteins, and just as these more complex biomolecules, it exhibits amide bands in the IR region.[29] By monitoring the amide I band position, it is possible to determine the secondary structure ($\alpha$-helix, $\beta$-sheet, or random coil).[25,29,30] Using time-resolved IR nanoscopy, the transition of the amide I band of one point on the PLL film can be followed during the change of its secondary structure.

## EXPERIMENTAL SECTION

**Sample Preparation.** Poly-L-lysine hydrobromide (MW 15.000−30.000) was purchased from Sigma-Aldrich. PLL films were prepared by spin-coating. Prior to film deposition, a $CaF_2$ substrate (Sigma-Aldrich) was subjected to cleaning by means of subsequent 10 min rinses in acetone, ethanol, and distilled water ultrasonic baths. An aqueous solution of PLL with concentration 4.6% (w/v) was used for the spin-coating procedure. One drop (3 $\mu$L) of the PLL solution was casted at the spinning substrate with rotation speed 1500 rpm and rotation time of 1 min. The topography of the prepared film was characterized by AFM. For all dynamic measurements, the $CaF_2$ substrate was placed on a thermo electric heater/cooler which was connected to a temperature controller.

**FTIR Spectroscopy.** FTIR spectra were collected in transmission mode at 4 $cm^{-1}$ resolution on a FTIR microscope (Hyperion 3000, BRUKER) with a liquid nitrogen cooled MCT detector. Every spectrum was averaged from 128 scans, with a sampling area of about 100 $\mu$m by 100 $\mu$m. Measurements were performed in homogeneous regions of the film with a thickness of about 200 nm. The absolute height of the film was obtained by introducing a scratch into the film down to the substrate and measuring the step height at the wall of the scratch with an AFM. Homogeneity of the film was checked by evaluation of the intensity of the amide I band. The absorption at arbitrary areas of measurement was nearly the same and the standard deviation was not larger than 7%.

The presence of water creates several artifacts in the IR spectra of proteins. The most prominent of these artifacts are water vapor bands and liquid water absorptions across the amide I band originating from a water HOH deformation band at ∼1640 $cm^{-1}$.[3] Usually, the water vapor bands are reduced by evacuating the path of the IR beam or flushing the measurement chamber with dry air. However, our experiments require a humid environment to perform the secondary structure change of the PLL film. This problem was overcome by using $D_2O$ instead of $H_2O$ to create humid air. The DOD deformation band is located at lower wavenumbers than the HOH deformation band (1208 $cm^{-1}$ as opposed to 1640 $cm^{-1}$),[31] allowing unperturbed protein spectroscopy in the amide I region.

Dynamic measurements were performed in a two-step process. First, the HD exchange was initiated by blowing dry air from an adsorption dryer (K-MT 2 MS/TE, AGRE, Austria) at a flow rate of 90 L/h through a washing flask with $D_2O$ over the sample. Then, with the air still running, the secondary structure change was initiated by changing the substrate temperature.

**PTIR Setup.** As outlined above, the setup consists of an IR light source for excitation of thermal expansion of the sample and a scanning probe microscope for spatially resolved detection of the thermal expansion. In this work, a Daylight solution EC-QCL with a peak power of 800 mW and tuning range from 1565 to 1720 $cm^{-1}$ was used as a light source in combination with an Agilent 5400 AFM with a MAC III controller as a detector. The manufacturer states a spatial drift in the range of 0.5 nm $min^{-1}$ when the instrument is at thermal equilibrium. A sketch of the setup is depicted in Figure 1. The system was placed onto an air dampened vibration isolation table to reduce the mechanical noise in the system.

A reflective optic consisting of gold mirrors (Thorlabs) was used to direct the laser beam from the source to the sample below the AFM cantilever. In addition to plane mirrors for redirecting the beam, a beam expander was added to reduce the divergence of the beam. An off-axis parabolic mirror was used to focus the light onto the sample. The beam expander consists of one parabolic mirror with 2″ and one with 6″ reflected focal


DOI: 10.1021/acs.analchem.5b00241
Anal. Chem. 2015, 87, 4415−4420

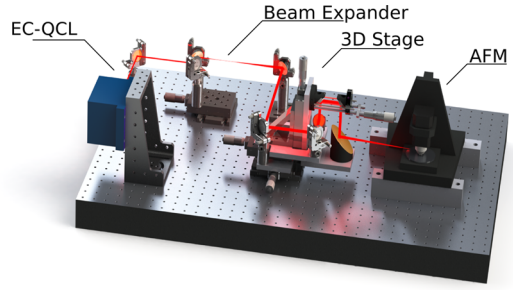


**Figure 1.** Sketch of the optical setup used for performing fast IR nanoscopy. The IR laser beam is shown in red. Not depicted: PE foil housing to allow controlling the atmosphere in the beam path and around the AFM (e.g., create water-vapor free, but $D_2O$-enriched environment).

length. A combination of three translation stages was used to move the position of the focal spot on the sample in three dimensions independently.

The AFM was placed slightly (50 mm) elevated from the optical table to allow for better optical access. Due to the small distance of about 2 mm between the sample and the AFM nose cone, the IR beam had to be directed onto the sample at an angle of incidence above 77°.

All IR nanoscopy measurements were performed using gold covered cantilevers HQ:CSC38/CR-AU (MikroMasch, US).

To reduce the influence of water vapor on the laser intensity, the setup was placed in a housing of polyethylene foil and constantly flushed with dry air. The sample was prepared as described above. Dry air humidified with deuterium oxide was blown across the sample as described for the FTIR experiments.

**Fast Spectra Acquisition.** For fast acquisition of the local IR absorption of the sample across the emission range of the EC-QCL, the sweep mode of the Daylight solution laser was used. In this mode, the grating of the laser is sweeped across a range of wavenumbers set at an approximately constant rate of wavenumbers per second. However, since the grating has to be accelerated at the starting wavenumber and decelerated at the stopping wavenumber, this rate is not constant across one sweep. To correct for deviations from the linear behavior, the laser sweep was characterized in step-scan measurement on an FTIR spectrometer (VERTEX 80v, BRUKER, Germany) as described elsewhere.[27,32]

The IR absorption was filtered from AFM deflection signal through the Agilent 5400 built-in lock-in amplifier. To trigger the emission of the EC-QCL at the frequency of the AFM 5400 lock-in amplifier the lock-in amplifier's sinusoidal reference signal had to be converted to a 5 V rectangular signal. The reference signal was set to an offset of 1.3 V and peak to peak amplitude of 2 V. A Schmidt trigger was used to convert the sinusoidal signal into rectangular pulses at the needed level which were fed to the TRIGGER input of the EC-QCL driver. The EC-QCL was operated in the external trigger mode in which the start of a pulse is determined by the positive edge on the TRIGGER input while the length of the pulse is set via the serial interface from a PC to the laser driver. These electronics suffice to perform single wavelength PTIR measurements and imaging.

However, to acquire local IR spectra the lock-in signal has to be recorded starting at the positive edge of the SCAN ENABLE pulse of the EC-QCL. Since external triggering of data collection is currently not possible with the Agilent hardware, the lock-in amplitude signal was instead output as an analog signal on one of the BNC connectors of the MAC III box and then digitized with a national instruments analog digital converter (ADC). The NI9401 digital I/O (National Instruments, US) was used to trigger the acquisition from the SCAN ENABLE signal. The lock-in filtered signal was output as an analog signal from the AFM controller and recorded using a NI9239 50kSs$^{-1}$ADC (National Instruments, US). A sketch of all electronic connections between the individual parts of the used setup is depicted in Figure 2.

To speed up the acquisition of spectra and the retuning of the repetition rate, a Python script was implemented that automatically measured spectra at given points across the sample. The interface to the national instruments card was done via PyDAQmx library,[33] the Daylight laser was controlled

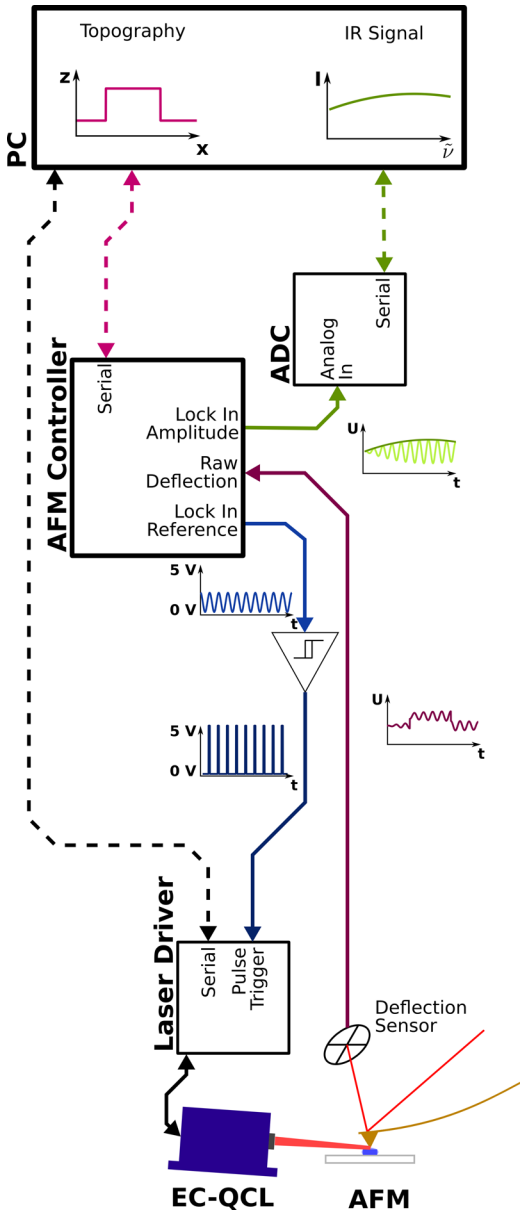


**Figure 2.** Sketch of the electronic connections in the setup used in this work. Solid lines are analog signals while dashed lines symbolize digital connections. The graphs in the sketch show the shape of the signals in the analog connections next to them (corresponding colors) and the final output displayed on the PC user interface.



DOI: 10.1021/acs.analchem.5b00241
*Anal. Chem.* 2015, 87, 4415−4420

via an in-house written Daylight laser controller which communicated with the laser via PyVISA. The AFM was controlled using the Python version of Picoscript provided by Agilent.

To remove high frequency modulations and to reduce noise in the raw data a Fourier transform based low-pass filter was applied to each collected sweep. To further improve the signal-to-noise ratio (SNR) several laser sweeps can be averaged at the cost of reducing time resolution.

**Resonance Tracking.** The signal in resonant PTIR spectroscopy strongly depends on the proximity of the repetition rate of the laser and the contact resonance, i.e. the mechanical resonance of the cantilever - sample system. The highest signal can be achieved, if the repetition rate of the EC-QCL is close to the resonance frequency of the system. In cases, when the repetition rate is far - in our system about 10 kHz or more - from the cantilever resonance, no photo-expansion signal can be detected at all. In systems with changing parameters (e.g., temperature) that lead to changing mechanical properties and resonance positions, the laser repetition rate has to be readjusted to the contact resonance in order to achieve the highest signal. In this system, the readjustment was achieved in a two step process. First, the amplitude of the cantilever was measured for a series of repetition rates across the frequency range wherein the resonance was expected to lie. From this measurement set, the repetition rate corresponding to the maximum amplitude was determined, which was then used for the laser scan. This procedure was performed prior to recording of each spectrum.

## RESULTS AND DISCUSSION

In a preliminary examination of the dynamic behavior of the sample, far-field FTIR transmission measurements of the PLL film prepared as described above were performed in a dry air environment.

FTIR measurements of the PLL thin film revealed the well-known amide I band in the region between 1600 and 1700 $cm^{-1}$ with the maximum at 1650 $cm^{-1}$ ($\alpha$-helix).[25,34] After adding $D_2O$ vapor to the air blown across the sample, a small shift in the position of the maximum of the band toward lower wavenumbers was observed (see Figure 3). This shift of the amide I band detected after HD exchange is due to replacement of hydrogen atoms in the polypeptide film by heavier deuterium atoms. The amide I band of a protein or polypeptide after HD exchange is usually called amide I′.

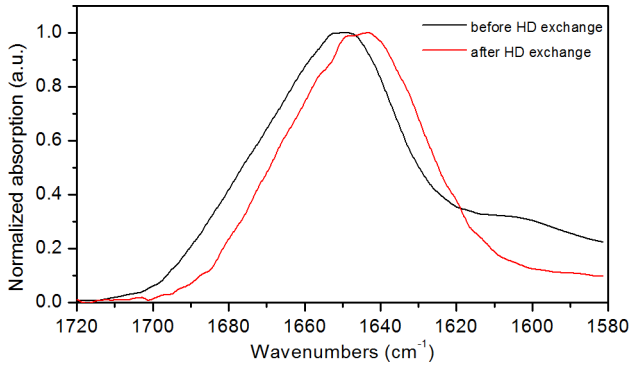


**Figure 3.** FTIR spectra of the PLL thin film deposited on $CaF_2$ substrate before and after HD exchange. Replacement of hydrogen by the heavier deuterium atoms leads to a shift of the amide I band to lower wavenumbers (amide I′).

The secondary structure change in the deuterated polypeptide was initiated by increasing the relative content of gaseous deuterium oxide in the PLL film (by increasing the degree of film hydration through decreasing the film temperature). As the (heavy) water content of the film is increased, the intramolecular hydrogen bonds in PLL are replaced by intermolecular hydrogen bonds between $D_2O$ and PLL, which leads to a change of the PLL secondary structure from $\beta$-sheet to $\alpha$-helix.[28] Figure 4 shows the time-resolved transfer from $\beta$-sheet to $\alpha$-helix secondary conformers measured in the FTIR experiment.

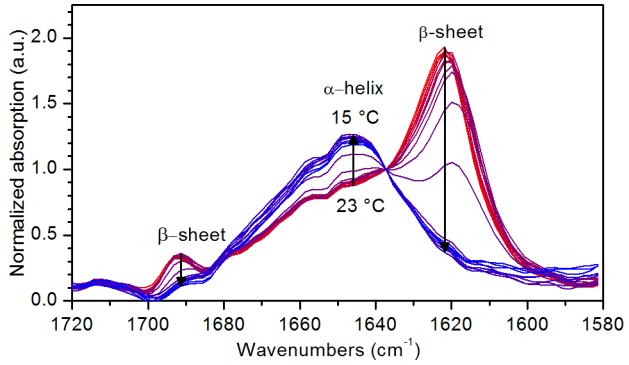


**Figure 4.** Time-resolved FTIR spectra of secondary structure change of the PLL thin film deposited on $CaF_2$ substrate during the HD exchange. When the temperature is decreased from 23 °C (red) to 15 °C (blue), the amide I′ bands corresponding to $\beta$-sheet secondary structure decrease and the one corresponding to the $\alpha$-helix arises instead.

While the substrate was cooled down from 23 to 15 °C over the course of 22 min, the amide I′ bands at 1614 and 1690 $cm^{-1}$, corresponding to $\beta$-sheet secondary structure, gradually decreased, concurring with the increase of a single band at 1650 $cm^{-1}$, indicating the emergence of $\alpha$-helix as the dominating secondary structure element.

The same transition was registered by PTIR nanoscopy: For this time-resolved near-field measurement, the PLL film sample was placed in the PTIR setup under a stream of dry air enriched with $D_2O$ vapor. The secondary structure change from $\beta$-sheet to $\alpha$-helix was again triggered by slowly decreasing the temperature of the sample from 25 to 23 °C over a period of 19 min. Time-resolved spectra of this transition are depicted in Figure 5.

During the temperature change the bands at ∼1618 and 1680 $cm^{-1}$ corresponding to the $\beta$-sheet decreased and the band at ∼1650 $cm^{-1}$ assigned to the $\alpha$-helix increased, as was also observed in the far-field measurements (Figure 4). While the same spectral features arising from the change in the polypeptide were observed (shown in Figure 5), PTIR exhibited a nonstructured but curved baseline that is not present in the FTIR spectra. We attribute this feature to a direct excitation of the cantilever by the laser. This direct excitation is proportional to the laser intensity and is independent of the infrared spectrum of the sample. The curve in this contribution stems from the wavelength dependence of the emitted intensity of the EC-QCL.

A time resolution of 67 s per measurement (average of 3 consecutive sweeps of the laser) proved to be sufficiently fast to


DOI: 10.1021/acs.analchem.5b00241
Anal. Chem. 2015, 87, 4415−4420

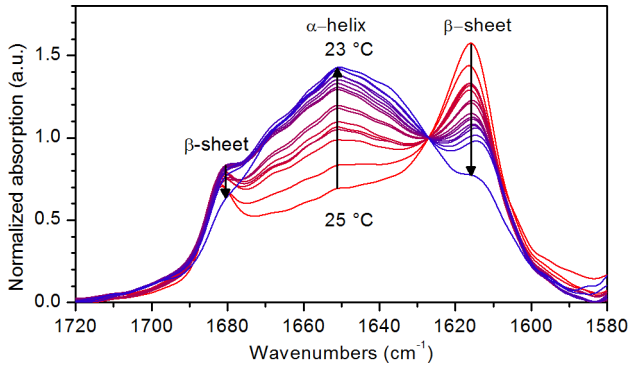


**Figure 5.** Time-resolved PTIR spectra of secondary structure change of the PLL thin film deposited on $CaF_2$. The full measurement series took 19 min. At the end of the series, the change from $\beta$-sheet to $\alpha$-helix secondary structure is mostly completed.

accurately resolve the spectral change in the amide I′ band. However, 67 s per spectrum is not the limit of the temporal resolution of the instrument. In a further experiment, a steeper temperature ramp was used to change the conformation of the PLL thin film in a faster manner (see Figure 6). In this

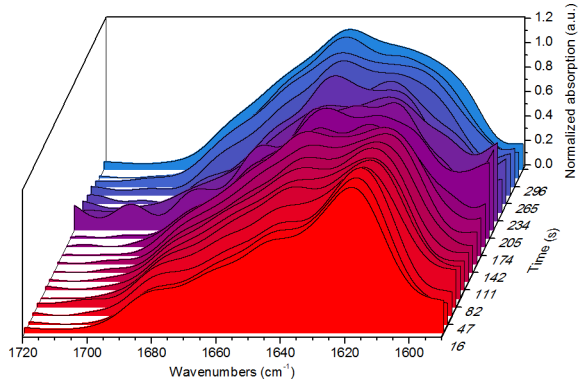


**Figure 6.** Time-resolved IR nanoscopy spectra of a PLL thin film taken every 15 s during a temperature ramp. The $z$-axis shows the time in seconds at which the measurement was taken. A change from $\beta$-sheet to $\alpha$-helix secondary structure occurs within 300 s. At an acquisition rate of 15 s per spectrum, this change can be clearly detected.

measurement series, the time difference between two spectra was set to the current maximum acquisition speed of the instrument of 15 s per measurement. These faster changes in the spectra were well-resolved using this higher acquisition rate (see Figure 6). The laser sweep by itself is completed within 1.5 s.

The remaining time needed for a single measurement is spent on retuning the lock-in amplifier to the contact resonance of the system, as described in the Experimental Section. This step is necessary, because alterations of the temperature in the system lead to changes of the mechanical properties. Figure 7 shows the resulting shift of the cantilever contact resonance frequency at different temperatures.

In this measurement setup, where the alteration of the temperature is necessary to initiate a reaction, retuning the lock-in is indispensable. To achieve higher temporal resolution, a better retuning method could be used,[35] which would limit the time resolution to the time of a single laser scan. For samples that do not undergo changes in the mechanical

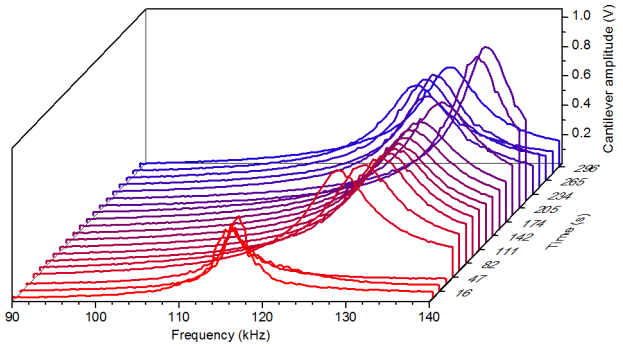


**Figure 7.** Lock-in amplitudes recorded during the tuning step of the measurement series in Figure 6. Differences in the resonance frequency make necessary retuning of the cantilever after each measurement.

properties during the reaction, retuning the lock-in amplifier is not necessary. In these cases we expect that an even better time resolution can be achieved with an approximate acquisition rate of one spectrum per 1.5 s with our setup. After removing this lock-in tuning procedure as a limiting factor, the laser scan time is a remaining limit on the time resolution. The laser scan time is a function of the EC-QCL scanning speed and the desired wavenumber range—which is often not open for discussion. Currently, commercially available EC-QCLs boast a scanning rate up to 1000 $cm^{-1}$ $s^{-1}$ which implies a scan time of the entire amide I region of about 100 ms. Of course, for the use of this fast tuning laser, other instrument parameters such as the frequency of the contact resonance and accordingly the laser repetition rate would also have to be adapted.

In addition to changes in the mechanical properties of the sample, the temperature change is also expected to lead to a spatial drift of the cantilever tip in excess of the rate of 0.5 nm $min^{-1}$ given for a system in thermal equilibrium. This drift was not considered relevant for this work for two reasons: first because only a small temperature change was needed to perform the experiment and second because the film was assumed to be homogeneous. If a higher lateral stability of the cantilever is needed, a closed-loop scanner could be used instead the open-loop scanner used in this work.

## CONCLUSION

PTIR is a promising technique for nondestructive chemical imaging of a multitude of samples. In this work, we demonstrated the feasibility of time-resolved PTIR measurements of nonrepeatable events at a wavenumber range of more than 100 $cm^{-1}$. Using a custom-made setup of commercially available parts, we followed the conformational change of PLL, initiated by changing the degree of hydration in the biological film. The spectra acquired with PTIR at a time resolution of 67 s per spectrum (3 scans) agree well with the ones taken with conventional FTIR microscopy. The maximum acquisition speed for this setup was determined to be 15 s per spectrum. A limiting factor is retuning of the lock-in amplifier. This procedure is necessary, because the temperature change used to induce the conformational change of the polypeptide alters the mechanical properties, causing the mechanical resonance to drift. It takes approximately 13.5 s to retune the lock-in. Without this tuning step, i.e. for measurements that do not involve changes in the sample temperature, acquisition speeds as high as 1.5 s per spectrum can be achieved.



DOI: 10.1021/acs.analchem.5b00241
*Anal. Chem.* 2015, 87, 4415−4420

In conclusion, the presented approach of time-resolved PTIR of nonrepeatable events at an expanded wavenumber range provides a missing piece in the toolbox of near-field imaging techniques, that complements the available subpicosecond time resolution achieved for repeatable events[21,24] and the well-established imaging of static samples. In the future, time-resolved IR nanoscopy may thus be of particular interest for a wide range of problems where chemical information is needed at a high spatial resolution as well as with temporal resolution. Potential systems of interest are the detection of chemical changes in a polymer during heat degradation,[16] the monitoring of hydration of polymer electrolyte membranes used for fuel cells[36] and analyzing chemical changes of wood under UV irradiation.[37]

## ■ ASSOCIATED CONTENT

### Supporting Information

Second derivative spectra of the first and last spectra in Figures 4 and 5 showing the band positions without background contributions. This material is available free of charge via the Internet at http://pubs.acs.org.

## ■ AUTHOR INFORMATION


### Corresponding Author

*E-mail: bernhard.lendl@tuwien.ac.at.


### Author Contributions

G.R. designed and built the PTIR setup used in this work. A.B. performed FTIR and PTIR measurements and sample preparation. G.R. evaluated the measurements. The paper was written jointly by G.R. and A.B. A.S. supported and advised G.R. and A.B. in composing this paper. B.L. served as supervisor for G.R. and A.B. for all parts of the work. The manuscript was written through contributions of all authors. All authors have read the final version of the manuscript.

## ■ ACKNOWLEDGMENTS


The authors would like to thank Dieter Baurecht (University of Vienna) for initial help with use of PLL as a model substance for proteins. Ferry Kienberger and Christian Rankl of Keysight Laboratories, Linz, Austria (formerly Agilent Laboratories), provided the AFM used in this work and provided help and advice throughout the experiments. Johannes Frank (TU Vienna) fabricated mechanical parts for the setup. The thermocontroller was built by Wolfgang Tomischko (TU Vienna). The work was supported financially by the Austrian Science Fund (FFG) projects No. 478599 and 465271 as well as the Ph.D. school MEIBio at TU Vienna.


## ■ REFERENCES


(1) Baker, M. J.; Trevisan, J.; Bassan, P.; Bhargava, R.; Butler, H. J.; Dorling, K. M.; Fielden, P. R.; Fogarty, S. W.; Fullwood, N. J.; Heys, K. a; Hughes, C.; Lasch, P.; Martin-Hirsch, P. L.; Obinaju, B.; Sockalingum, G. D.; Sulé-Suso, J.; Strong, R. J.; Walsh, M. J.; Wood, B. R.; Gardner, P.; Martin, F. L. *Nat. Protoc.* **2014**, *9*, 1771−1791.

(2) Surewicz, W. K.; Mantsch, J. H. H.; Chapman, D. *Perspect. Biochem.* **1993**, *32*, 329−394.

(3) Kong, J.; Yu, S. *Acta Biochim. Biophys. Sin. (Shanghai)* **2007**, *39*, 549−559.

(4) Sahu, R. K.; Mordechai, S. *Future Oncol.* **2005**, *1*, 635−647.

(5) Lasch, P.; Naumann, D. *Biochim. Biophys. Acta* **2006**, *1758*, 814−829.

(6) Ocelic, N.; Huber, A.; Hillenbrand, R. *Appl. Phys. Lett.* **2006**, *89*, 101124.

(7) Brehm, M.; Taubner, T.; Hillenbrand, R.; Keilmann, F. *Nano Lett.* **2006**, *6*, 1307−1310.

(8) Dazzi, A.; Prazeres, R.; Glotin, F.; Ortega, J. M. *Opt. Lett.* **2005**, *30*, 2388.

(9) Dazzi, A.; Prater, C. B.; Hu, Q.; Chase, D. B.; Rabolt, J. F.; Marcott, C. *Appl. Spectrosc.* **2012**, *66*, 1366−1384.

(10) Huth, F.; Govyadinov, A.; Amarie, S.; Nuansing, W.; Keilmann, F.; Hillenbrand, R. *Nano Lett.* **2012**, *12*, 3973−3978.

(11) Lu, F.; Jin, M.; Belkin, M. A. *Nat. Photonics* **2014**, *8*, 307−312.

(12) Amenabar, I.; Poly, S.; Nuansing, W.; Hubrich, E. H.; Govyadinov, A. a; Huth, F.; Krutokhvostov, R.; Zhang, L.; Knez, M.; Heberle, J.; Bittner, A. M.; Hillenbrand, R. *Nat. Commun.* **2013**, *4*, 2890.

(13) Lahiri, B.; Holland, G.; Centrone, A. *Small* **2013**, *9*, 488.

(14) Deniset-Besseau, A.; Prater, C. B.; Virolle, M.-J.; Dazzi, A. *J. Phys. Chem. Lett.* **2014**, *5*, 654−658.

(15) Policar, C.; Waern, J. B.; Plamont, M. A.; Clède, S.; Mayet, C.; Prazeres, R.; Ortega, J. M.; Vessières, A.; Dazzi, A. *Angew. Chem., Int. Ed.* **2011**, *50*, 860−864.

(16) Marcott, C.; Lo, M.; Kjoller, K.; Prater, C.; Noda, I. *Appl. Spectrosc.* **2011**, *65*, 1145−1150.

(17) Katzenmeyer, A. M.; Chae, J.; Kasica, R.; Holland, G.; Lahiri, B.; Centrone, A. *Adv. Opt. Mater.* **2014**, *2* (8), 718−722 DOI: 10.1002/adom.201400005.

(18) Katzenmeyer, A. M.; Canivet, J.; Holland, G.; Farrusseng, D.; Centrone, A. *Angew. Chem., Int. Ed.* **2014**, *53*, 2852−2856.

(19) Chen, J.; Badioli, M.; Alonso-González, P.; Thongrattanasiri, S.; Huth, F.; Osmond, J.; Spasenović, M.; Centeno, A.; Pesquera, A.; Godignon, P.; Zurutuza Elorza, A.; Camara, N.; de Abajo, F. J. G.; Hillenbrand, R.; Koppens, F. H. L. *Nature* **2012**, 3−7.

(20) Fei, Z.; Rodin, a. S.; Andreev, G. O.; Bao, W.; McLeod, a. S.; Wagner, M.; Zhang, L. M.; Zhao, Z.; Thiemens, M.; Dominguez, G.; Fogler, M. M.; Neto, a. H. C.; Lau, C. N.; Keilmann, F.; Basov, D. N. *Nature* **2012**, *487*, 82−85.

(21) Wagner, M.; Fei, Z.; McLeod, A. S.; Rodin, A. S.; Bao, W.; Iwinski, E. G.; Zhao, Z.; Goldflam, M.; Liu, M.; Dominguez, G.; Thiemens, M.; Fogler, M. M.; Castro Neto, A. H.; Lau, C. N.; Amarie, S.; Keilmann, F.; Basov, D. N. *Nano Lett.* **2014**, *14*, 894−900.

(22) Schnell, M.; Garcia-Etxarri, A.; Huber, A. J.; Crozier, K. B.; Borisov, A.; Aizpurua, J.; Hillenbrand, R. *J. Phys. Chem. C* **2010**, *114*, 7341−7345.

(23) Taubner, T.; Hillenbrand, R.; Keilmann, F. *Appl. Phys. Lett.* **2004**, *85*, 5064−5066.

(24) Wagner, M.; McLeod, A. S.; Maddox, S. J.; Fei, Z.; Liu, M.; Averitt, R. D.; Fogler, M. M.; Bank, S. R.; Keilmann, F.; Basov, D. N. *Nano Lett.* **2014**, *14*, 4529−4534.

(25) Barth, A. *Biochim. Biophys. Acta* **2007**, *1767*, 1073−1101.

(26) Brandstetter, M.; Genner, A.; Anic, K.; Lendl, B. *Analyst* **2010**, *135*, 3260−3265.

(27) Ramer, G.; Kasberger, J.; Brandstetter, M.; Saeed, A.; Jakoby, B.; Lendl, B. *Appl. Phys. B: Laser Opt.* **2013**, *116*, 325−332.

(28) Prestrelski, S. J.; Tedeschi, N.; Arakawa, T.; Carpenter, J. F. *Biophys. J.* **1993**, *65*, 661−671.

(29) Szyc, Ł.; Pilorz, S.; Czarnik-Matusewicz, B. *J. Mol. Liq.* **2008**, *141*, 155−159.

(30) Kong, J.; Yu, S. *Biochemistry* **2007**, *39*, 549−559.

(31) Bertie, J. E.; Ahmed, M. K.; Eysel, H. H. *J. Phys. Chem.* **1989**, *93*, 2210−2218.

(32) Brandstetter, M.; Lendl, B. *Sensors Actuators B Chem.* **2012**, *170*, 189−195.

(33) Cladé, P. PyDAQmx: a Python interface to the National Instruments DAQmx driver. http://pythonhosted.org/PyDAQmx/.

(34) Dzwolak, W.; Smirnovas, V. *Biophys. Chem.* **2005**, *115*, 49−54.

(35) Sonnaillon, M. O.; Bonetto, F. J. *Rev. Sci. Instrum.* **2007**, *78*, 014701.

(36) Kunimatsu, K.; Bae, B.; Miyatake, K.; Uchida, H.; Watanabe, M. *J. Phys. Chem. B* **2011**, *115*, 4315−4321.

(37) Müller, U.; Rätzsch, M.; Schwanninger, M.; Steiner, M.; Zöbl, H. *J. Photochem. Photobiol. B Biol.* **2003**, *69*, 97−105.




DOI: 10.1021/acs.analchem.5b00241
*Anal. Chem.* 2015, 87, 4415−4420